 doi:10.20944/preprints202009.0203.v1

Article

A Comparative Study on the Properties of Cu-Cr-Mo System Electrical Contact Material by Sintering and Infiltration Method

Yeong Woo Cho[1,2], Jae Jin Sim[1,2], Sung Gue Heo[1], Jong Soo Byeon[1,2], Kee Ahn Lee[2], Taek-Soo Kim[1], Seok-Jun Seo[1], Heung Jin Ju[3], Kyoung Tae Park[1,*]

[1] Korea Institute of Industrial Technology, Tower to Get Pearl, Gaetbeol-ro 12, Yeonsu-gu, Incheon, Republic of Korea 1; kicho20@kitech.re.kr
[2] In-Ha University, 100, Inha-ro, Michuhol-gu, Incheon, Republic of Korea 2
[3] VITZRO EM Co., Ltd, 327, Byelmang-ro, Danwon-gu, Ansan, Republic of Korea 3
* Correspondence: ktpark@kitech.re.kr Tel.: +82-10-5728-9588

Abstract: The contact materials in high-voltage vacuum interrupter require properties such as high conductivity, high density, and high hardness to minimize arc heat damage. In this study, copper–molybdenum-chromium alloys contact materials are examined for a high voltage contact material. Ball milling process was carried out after analyzing the raw materials of copper, chromium, and molybdenum powders. A green compact was produced using a high press with the mixed powder. Afterwards, composite was produced by sintering method according to temperature and infiltration method according to Cu content in green compact. The composite of sintering method showed a density of 8.55 g/cm3 (relative density 93%) a hardness of 217 HV, and an electrical conductivity of 40.7 IACS% at 1200 °C. The composite of 10 wt.% Cu produced by the Cu infiltration method showed a density of 8.7 g/cm3 (relative density 94%), Hardness of 274HV and electrical conductivity of 39 IACS% at 1300 °C. The measurements of physical properties showed the new possibility of using the Cu–Cr–Mo alloy as a contact material for high-voltage vacuum interrupters.

Keywords: Electrical contact material; Cu–Cr–Mo; Liquid phase sintering; Infiltration method; Hardness; Electrical conductivity

1. Introduction

The insulation and arc extinction properties during a contact operation are important for contact materials used in high-voltage vacuum interrupters, and the mechanical properties of the electrical contact materials are critical in meeting their requirements. If arc occurs during the on/off operation of the electrical contact point, arc heat causes local melting of the material surface, resulting in damage and breakage at the contact point. Since materials require thermal and electrical conductivity, high hardness, and high density to avoid damage from arc heat, two or more materials must be combined [1-3].

Copper (Cu) is a critical material in power devices due to its outstanding thermal and electrical conductivity, corrosion resistance, and excellent machinability. However, Cu has low hardness and limited industrial applications due to segregation that takes place during solidification. The hardness of Cu could be increased by adding an alloy element, but this could reduce its conductivity. Therefore, in order to maintain high conductivity, copper and insoluble alloying elements should be added [4]. Chromium (Cr) and Molybdenum (Mo) have a high melting point, so they have excellent workability even at high temperatures. Very fine and uniform Cr-Mo in Cu-matrix interface can provide properties such as high strength, fracture toughness, good ductility and corrosion resistance. In addition, Cr and Mo can be made stable alloys in the Cu–Cr–Mo system. This is because Cr and Mo is a homogeneous solid solution with a BCC crystal structure, same number of valence electrons,

Preprints (www.preprints.org) | NOT PEER-REVIEWED | Posted: 9 September 2020 doi:10.20944/preprints202009.0203.v1

and similar chemical properties. If mixed in any ratio, Cr–Mo exists as a single phase even at high temperatures [5-7]. The widely used manufacturing methods of contact materials such as the Cu–Cr system and the copper–tungsten (Cu–W) system include melting, infiltration, and sintering. During the melting process all metals are melted in a vacuum, but a large difference in the melting point between metals could potentially result in a non-uniform structure during the solidification process even if they become a uniform liquid phase. Hence, it is technically very difficult to obtain a uniform dispersion of metals by the melting method [8-12].

Therefore, this study produced a green compact by mixing raw materials and pressurizing them to produce Cu–Cr–Mo system contact materials. Then, we compared a composite made by the liquid phase sintering of the Cu–Cr–Mo mixture and a composite made by the infiltration of Cu into the Cr–Mo–Cu green compact body. The X-ray and microstructure of composite materials and their important mechanical properties including electrical conductivity, hardness, and density were analyzed.

2. Materials and Methods

2.1. Materials

Figure 1 shows scanning electron microscopy (SEM) images of raw materials of Cu (Avention^{Co}, 99.9% purity, 28 μm average particle size), Cr (Avention^{Co}, 99.9% purity, 27 μm average particle size), and Mo (Avention^{Co}, 99.9% purity, 20 μm average particle size) composite powders generated by sintering and infiltration.

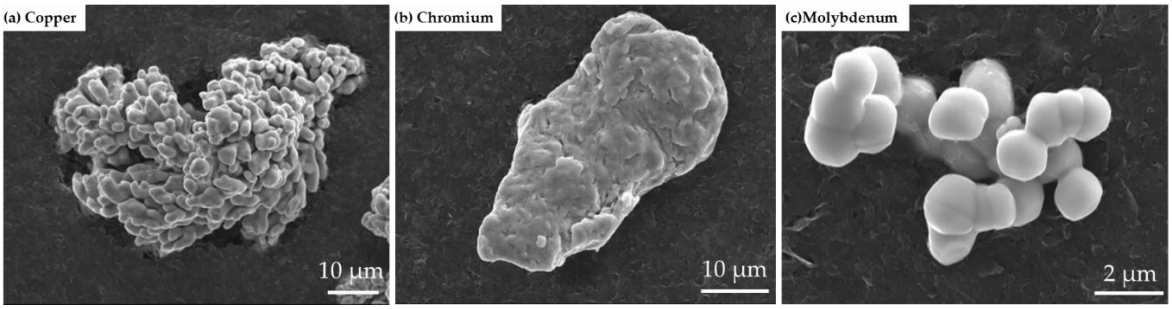

Figure 1. SEM images showing powders used in the study: (a) Cu (b) Cr and (c) Mo.

2.2. Experimental process

The sintering method (case (a)) of composite is represented in **Figure 2(a)**. For the sample preparation of the liquid phase from the Cu–Cr–Mo mixture, sintering was done by mixing each powder with 60 wt.%Cu – 30 wt.%Mo – 10 wt.%Cr, followed by ball mill mixing at 200 rpm for 4 h with a ball to material ratio of 5:1. Then, the mixed powder was loaded into a steel mold and pressurized at 148.5 MPa for 210 s to produce an 82 mm diameter green compact. After putting the green compact into an alumina crucible, it was heated at a rate of 10 °C/min and maintained at 1100 °C and 1200 °C for 3 h under Ar atmosphere.

The infiltration method (case (b)) of Cu into the Cr–Mo–Cu green compact is represented in **Figure 2(b)**. The ball mill mixture and green compact were created under the same conditions as the sintering process after mixing 10 wt.%Cr – 30 wt.%Mo – 10 wt.%Cu (50 wt.% Cu block) and 10 wt.%Cr – 30 wt.%Mo – 30 wt.%Cu (30 wt.% Cu block) powders. Then, to fill the remaining Cu content, Cu blocks (99.9% purity, 82mm diameter) were placed on top of the green compact and put in a graphite mold (inner diameter, 82 mm). The infiltration process was performed for 3 h at 1300 °C under Ar atmosphere at a heating rate of 8 °C/min without pressure.

Preprints (www.preprints.org) | NOT PEER-REVIEWED | Posted: 9 September 2020 doi:10.20944/preprints202009.0203.v1

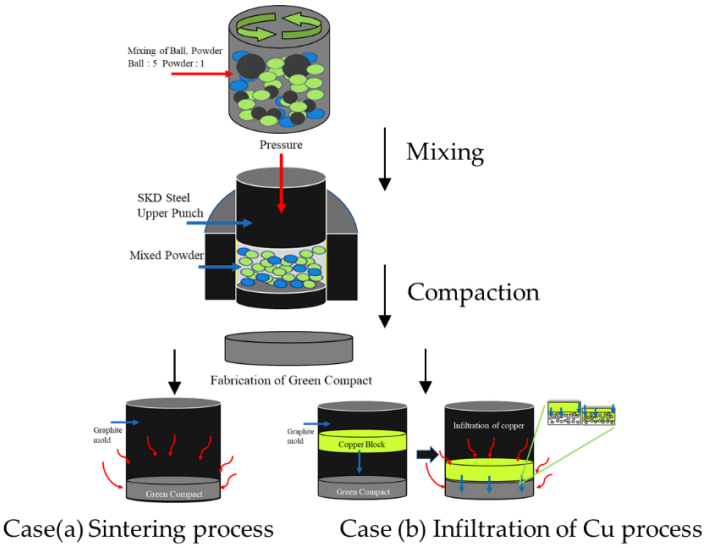

Figure 2. Schematic diagram of: case(a) the sintering, and case(b) infiltration of Cu processes.

2.2. Analysis technique

The density of composites produced by the sintering and infiltration processes was measured using the Archimedes method as shown in Eq. (1) where ρ is density, W_a is the weight of the sample in air, W_l is the weight of the sample in liquid, and ρ_l is liquid density.

$$\rho = \frac{W_a}{W_a - W_l} \times \rho_l \quad (1)$$

Hardness was measured by pressurizing the composites for 10 s with a test load of 0.1 kgf using a Vickers hardness tester (Mitutoyo, HM210A) as represented by Eq. (2) where F is the test load (kgf), S the diameter of the penetrator (mm), d the average diagonal of indentation (mm), and θ the face angle of the diamond indenter (136°).

$$HV = \frac{F}{S} = \frac{2F\sin\frac{\theta}{2}}{d^2} = 1.8544\frac{F}{d^2} \quad (2)$$

Electrical conductivity was analyzed by passing an eddy current across a cross-section using an electric conductivity meter (SIGMASCOPE, SMP350). The electric conductivity was calculated in %IACS (International Annealed Copper Standard) as shown in Eq. (3), where $\rho_{material}$ is the electrical conductivity (MS/cm), $\rho_{pure\ copper}$ is the resistivity (μΩ·cm)

$$\%(IACS) = \frac{1}{\rho_{material}} \times \rho_{pure\ copper} \quad (3)$$

Microstructure of composite and quantitative evaluation of the present impurities was observed through scanning electron microscopy/energy-dispersive X-ray spectroscopy (SEM/EDS, JEOL, JSM-7100F) and X-ray diffraction (XRD, BRUKER AXS, D8 ADVANCE) after mechanical polishing of the composite surface.

3. Results and discussion

3.1. Materials

Figure 3 shows EDS images of Cu, Cr, and Mo material powders mixed by ball milling. The SEM–EDS analysis showed that the powders were combined, and the shape of the Cu particle changed from coral to plate due to ball milling as Cu has higher ductility than Mo and Cr. Mo particle diameter was separated to less than 5 μm. In many studies on milling, the mixing time was crucial

Preprints (www.preprints.org) | NOT PEER-REVIEWED | Posted: 9 September 2020 doi:10.20944/preprints202009.0203.v1

and increasing the mixing time could result in more homogeneous particles and stability and refinement of materials during post-processing [12-14].

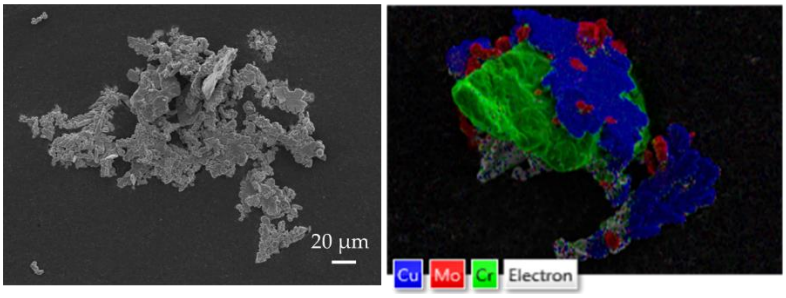

Figure 3. SEM–EDS image of Cu–Cr–Mo after ball milling.

3.2. Shrinkage

Photographs of macroscopic features of composites produced by sintering and Cu infiltration methods are shown in **Figure 4**. The heat treatment temperature was varied for both methods because Cu came out of the green compact and the shape was not maintained when the sintering temperature was set at 1300 °C. Therefore, the sintering temperature was set to 1100–1200 °C, given the fluidity of Cu in liquid phase, and to 1300 °C for the infiltration method. The four composites that were produced showed decreased diameters after the heat treatment process. The reason is that sintering at a temperature higher than Cu's melting point transformed the dispersed solids into liquid phase, causing shrinkage through the pulling force of the particles. Furthermore, the composite was contracted horizontally because it received more vertical pressure than horizontal pressure during the green compact fabrication process [15]. Based on the shrinkage ratio analysis, the 1200 °C sample generated by the sintering method had the largest diameter shrinkage ratio of approximately 9%, followed by the composite of 1300 °C 30 wt.% Cu, composite of 1100 °C and composite of 1300 °C 10 wt.% Cu as shown in **Table 1**.

Figure 4. Actual shapes of composites that were produced via sintering - case (a) and infiltration - case (b) methods: (a)1100 °C for 3h, (b) 1200 °C for 3h, (c) 10 wt.% Cu at 1300 °C for 3h, and (d) 30 wt.% Cu at 1300 °C for 3h.

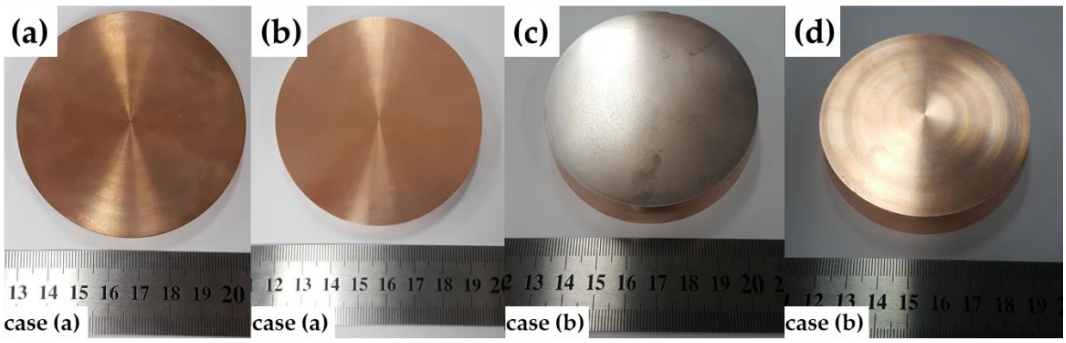

Process	Sample No.x		Composition (wt%)	Heat treatment temperature (℃)	Shrinkage rate (%)
Sintering	Case (a)	Sample (No. 1)	60Cu–10Cr–30Mo	1100	3
		Sample (No. 2)	60Cu–10Cr–30Mo	1200	9

Preprints (www.preprints.org) | NOT PEER-REVIEWED | Posted: 9 September 2020 doi:10.20944/preprints202009.0203.v1

Infiltration	Case (b)	Sample (No. 3)	10Cu–10Cr–30Mo + 50 Cu block	1300	1
		Sample (No. 4)	30Cu–10Cr–30Mo + 30 Cu block	1300	5

Table 1. Shrinkage rates of composites produced by sintering and infiltration methods

3.3. Sintering (case (a))

To investigate the alloying and impurities of the composite produced by the sintering method, a study was conducted using X-ray diffraction. **Figure 5** shows the XRD patterns in the composite produced by 1100 °C and 1200 °C according to the temperature by liquid sintering. The diffraction shows the peaks of the Cu phase and the Mo-Cr phase. The composite sintered at 1100 °C (sample no.1) has a lower diffraction intensity of the Mo-Cr phase than the composite of 1200 °C(sample no.2). Because the temperature was low, the sintering between Mo-Cr interface was not sufficiently performed, it shows that the intensity is low and the full width at half maximum (FWHM) is broad.

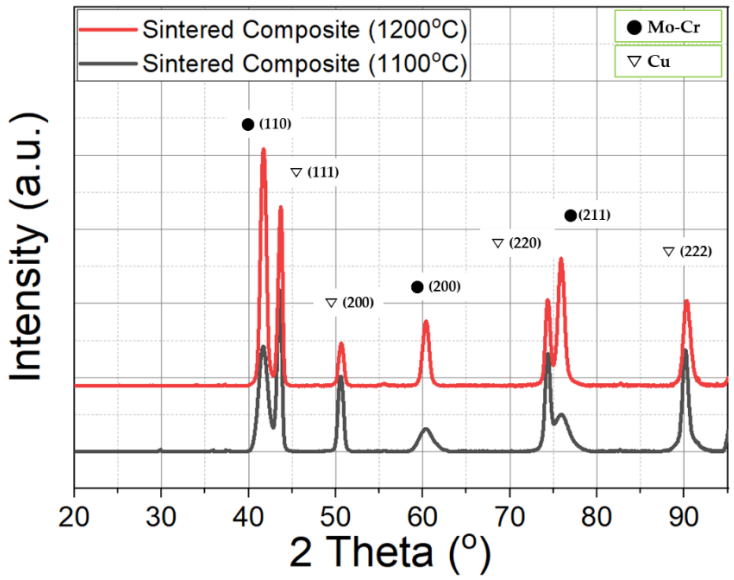

Figure 5. XRD of composites produced by the sintering method.

Figure 6 shows the SEM/EDS images of the microstructure of the 60 wt.%Cu–10 wt.%Cr–10 wt.%Mo composite produced by the sintering method. When the microstructure of the 1100 °C composite was examined, large pores were observed. There was not enough Cu in the high-viscosity liquid at 1100 °C; that is why the unstable flow of copper melt resulted in segregation. In contrast, it was found that in the microstructure of the 1200 °C composite, Cu, Cr, and Mo were uniformly distributed with no large pores and little segregation. [15, 24].

Preprints (www.preprints.org) | NOT PEER-REVIEWED | Posted: 9 September 2020 doi:10.20944/preprints202009.0203.v1

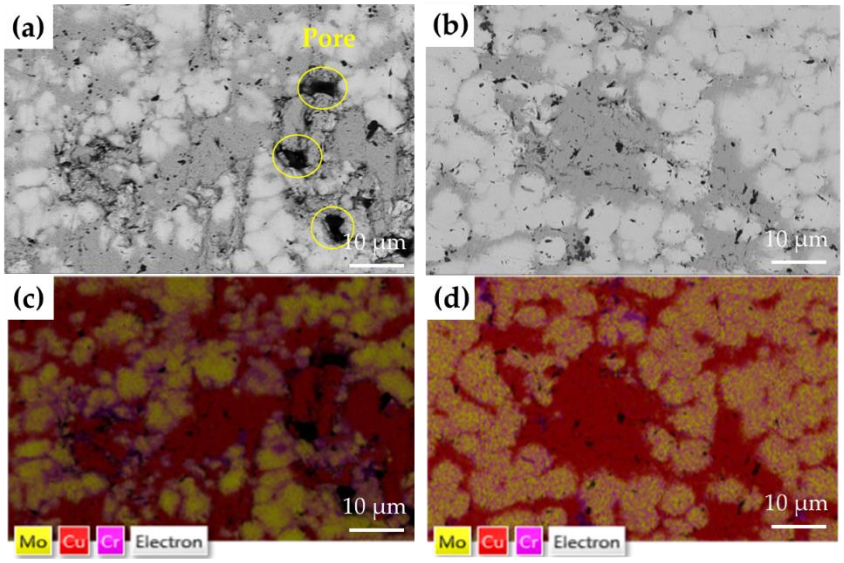

Figure 6. SEM/EDS images of microstructures of composites produced by the sintering method: (a) and (c) 1100 °C for 3h; (b) and (d) 1200 °C for 3h.

Figure 7 shows the density, conductivity, and hardness of composites produced by the sintering method. The composite that was kept at a sintering temperature of 1100 °C for 3h showed a density of 7.0 g/cm3 (relative density: 73%), an electrical conductivity of 25 %IACS, and a hardness of 152 HV (sample no. 1). The composite that was kept at a sintering temperature of 1200 °C for 3h showed a density of 8.55 g/cm3 (relative density: 93%), a conductivity of 40.7% IACS, and a hardness of 217 HV (sample no. 2) thus having properties with higher values. The reason is that although the melting point of Cu is 1083 °C, the Cu phase is not sufficiently liquidized at 1100 °C, resulting in an unstable bulk body and many pores. Furthermore, impurities present in the powder, including organic phases, evaporate at high temperatures, creating expansion and the formation of pores. When the sintering temperature was gradually increased, Cu is fully melted, and the viscosity of liquid Cu is decreased, which further promotes the sufficient rearrangement of Cr-Mo particles. This means that high temperatures contribute significantly to improving the degree of densification [15-18].

Not only does the formation of pores reduce density, but also because the Cu network is not properly distributed around the pores, electron movement in the Cu is obstructed, thus adversely affecting conductivity. The electrical resistance increased rapidly when the actual pore size increased, but on the other hand it was negligibly affected by the pore size when the pore size was sufficiently small [23]. Thus, when the temperature is 1200 °C rather than 1100 °C, the conductivity is higher due to the uniform distribution of Cu and the small number of pores with smaller size.

If the composition content is the same, there is a higher hardness at a higher sintering temperature. Hardness is correlated with density, and it is believed that pores cause stress condensation and low density. Thus, the temperature for densification of sintering is advantageous at 1200 °C rather than 1100 °C. It is clear that the homogeneous microstructure of composites sintered at higher temperatures leads to high physical properties. [24].

Preprints (www.preprints.org) | NOT PEER-REVIEWED | Posted: 9 September 2020 doi:10.20944/preprints202009.0203.v1

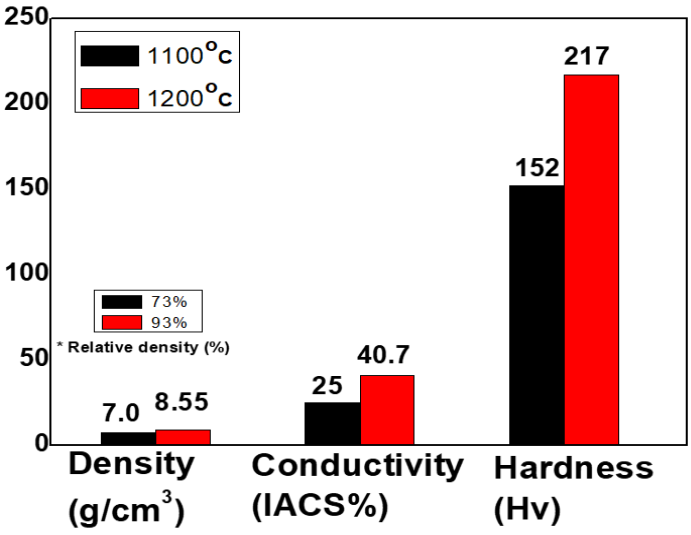

Figure 7. Comparison of mechanical properties (density, electrical conductivity, hardness) of composites produced by sintering 60 wt.%Cu – 10 wt.%Cr – 30 wt.%Mo.

3.4. Infiltration (case (b))

The infiltration method requires the green compact to have low density because its efficiency depends on pore volume. However, though pore volume is important, adequate pressurization is also important because maintaining the shape of the green compact is critical. In this study, the green compact was pressurized at 148.5 MPa, and the shape could not be maintained if it was pressurized below this pressure. Also, the Cr–Mo green compact without Cu did not maintain its shape as well.

The XRD pattern of the composite produced by infiltrating Cu bulk in a green compact with a Cu content of 10 wt.% Cu composite (sample no. 3) and 30 wt.% Cu composite (sample no. 4) is shown in **Figure 8**. The diffraction shows the peaks of the Cu phase and the Mo-Cr phase. Both composite did not show peaks of other compounds. The intensities of Cu peak (220) at 74.14 exhibited sample no. 4 contained higher Cu contents compared with sample no. 3.

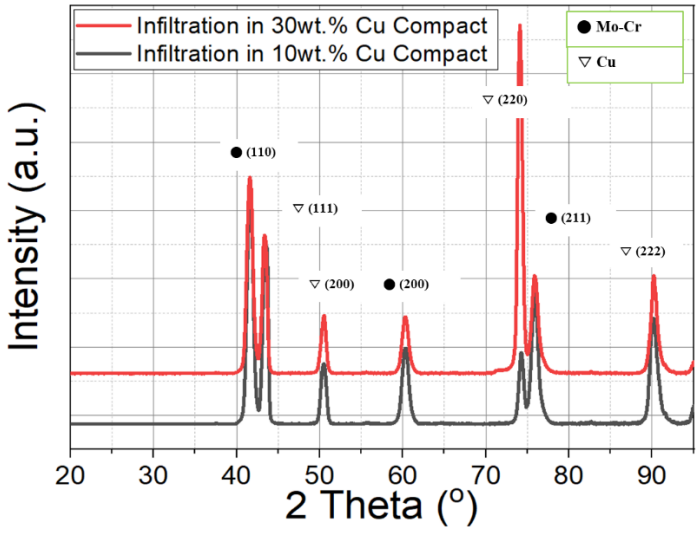

Figure 8. XRD of composites produced by the infiltration method.

Figure 9 shows SEM images of the microstructure of 10 wt.% Cu and 30 wt.% Cu composites produced by the infiltration method. The dark gray represents the Cu area and the bright gray represents the Cr–Mo area. Traces of infiltration can be found in the microstructure of 10 wt.% Cu, and the distribution of some Cu is non-uniform. The microstructure of 30 wt.% Cu composites have

Preprints (www.preprints.org) | NOT PEER-REVIEWED | Posted: 9 September 2020 doi:10.20944/preprints202009.0203.v1

a relatively uniform distribution of Cu, but has a higher number of pores. The uniform distribution and high content of Cu can improve the conductivity, but the pores can reduce the density [10].

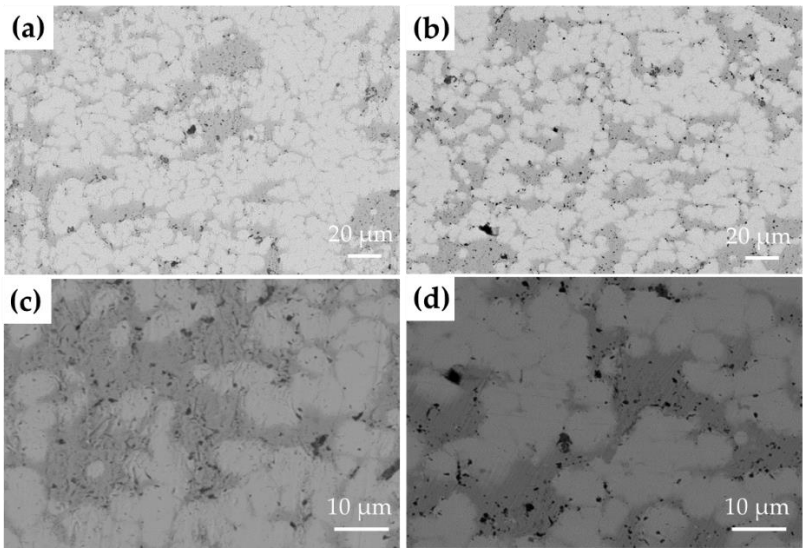

Figure 9. SEM images of microstructures of composites produced by the infiltration method. (a),(c): 10 wt.% Cu (sample no. 3) and (b), (d): 30 wt.% Cu (sample no. 4).

Figure 10 shows the density, electrical conductivity, and hardness of the composites generated by the infiltration method. The 10 wt.% Cu composite that was kept at a sintering temperature of 1300 °C for 3h showed a density of 8.7 g/cm3 (relative density 94%). The 30 wt.% Cu composite showed a density of 8.2 g/cm3 (relative density 89%). The 10 wt.% Cu composite had a slightly higher density than that of the 30 wt.% Cu composite. It seems that open pores in green compacts of the sample with 10 wt.% Cu were more secured than in that of the 30 wt.% Cu sample. Also, in the 30 wt.% Cu composite, it was observed that some Cu flowed out after the end of the experiment. It is ascribed that the Cu content in the green compact flowed out due to pressure by Cu block. This is understood to be a phenomenon caused by the high Cu content, which results in a greater rate of escape than the infiltration rate in the liquid phase process. The large pores of sample. no 4 observed in the SEM image are also judged to be the result of this, and the low relative density of the sample no. 4 is also described as the result of the formation of these pores. Thus the 10 wt. % Cu composite achieved higher relative density because the pore size was significantly lower.

The sintered composite from green compacts with 10 wt.% of copper contained showed lower electrical conductivity than that with 30 wt.% copper. The 30 wt.% Cu composite (sample no. 4) showed higher electrical conductivity. This is because the electrical conductivity depends on the distribution and content of Cu. The 30 wt.% Cu green compact has a higher Cu content between Mo-Cr contacts than the 10 wt.% Cu green compact. Thus, the electrical conductivity of 30 wt.% Cu composite (sample no. 4), which is uniformly distributed after Cu infiltration, was found to be higher despite larger pore size [18-20].

In the case of hardness of a composite, it is expected that Mo–Cr compositional ratio in green compacts is more predominant because the ratio of Mo–Cr in 10 wt.% Cu is relatively higher than 30 wt.% Cu in the process of making the green compact. Also the high density of the sintered composite is the main reason for high hardness. Therefore, the 10 wt.% Cu composite (sample no. 3) was considered to have a high hardness [21-25].

Preprints (www.preprints.org) | NOT PEER-REVIEWED | Posted: 9 September 2020 doi:10.20944/preprints202009.0203.v1

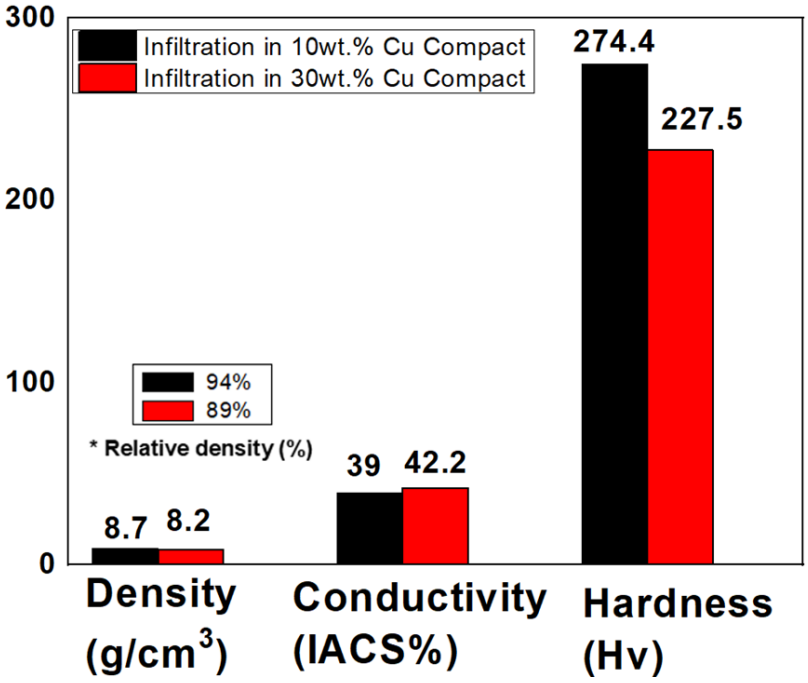

Figure 10. Comparison of the mechanical properties (density, electrical conductivity and hardness) of the composites produced by the infiltration method, depending on the amount of Cu added in the green compact.

4. Conclusions.

In this study, Cu–Cr–Mo system alloys were produced using liquid phase sintering and infiltration methods to develop high-voltage vacuum interrupter contact materials. The mechanical properties, which are required of contact materials, such as density, hardness, electrical conductivity, and microstructures were compared and analyzed. As a result, the following conclusions were reached:

1) Shrinkage with a reduced diameter occurred for composites produced using sintering and infiltration methods. Approximately 9% shrinkage was observed when the composites were maintained at 1200 °C for 3 h in the sintering method.
2) The density, electrical conductivity, and hardness of the composite produced by sintering method generated better properties at a sintering temperature of 1200 °C (sample no. 2) than at 1100 °C (sample no. 1).
3) Large pores were found in the microstructure of composite at a sintering temperature of 1100 °C (sample no. 1). These composite at sintering temperature of 1200 °C (sample no. 2) had a relatively homogeneous structure due to the sufficient liquefaction of Cu.
4) For composites made using the Cu infiltration method, 10 wt.% Cu (sample no. 3) had higher density and hardness, while 30 wt.% Cu (sample no. 4) had higher electrical conductivity.
5) In the microstructure of the 10 wt.% Cu composite (sample no. 3) produced by the infiltration method, some segregation was observed due to infiltration, and the microstructure of the 30 wt.% Cu composite (sample no. 4) had a uniform Cu distribution, but the number of pores increased.
6) Composites produced by the infiltration method have better mechanical properties compared to composites produced by the sintering method.
7) The measurements of mechanical properties showed the new possibility of using the Cu–Cr–Mo alloy as a contact material for high-voltage vacuum interrupters, and further research on this topic is needed.

6. Patents

Acknowledgments: This study was supported by the Korea Institute of Energy Technology Evaluation and Planning (KETEP) and the Ministry of Trade, Industry & Energy (MOTIE) of the Republic of Korea(No. 20165010100870) and the Korea Technology and Information Promotion Agency for SMEs(TIPA) and the Ministry of SMEs and Startups of the Republic of Korea(No.S2761733).

References

1. [1] Slade, P.G. IEEE T. Comp. Pack. Man **1994**, 17, 96
2. [2] Doh, J.M.; Park, J.K.; Kim, M.J. US Patent No. 6,551,374, Method of controlling the microstructures of Cu-Cr-based contact materials for vacuum interrupters and contact materials manufactured by the method **2003**
3. [3] Miao, B. Proc. ISDEIV, XXIst International Symposium on, IEEE **2004**, Yalta 2, 311
4. [4] Smith, W.F. Structure and Properties of Engineering Alloys, McGraw-Hill, New York, **2015**, pp. 239-291
5. [5] Aguilar, C.; Guzmán, D.; Castro, F.; Martínez, V.; de las Cuevas, F. Mater. Chem. Phys **2014**, 146, 493
6. [6] Kumar, A.; Pradhan, S.K.; Jayasankar, K.; Debata, M.; Sharma, P.K. J. Electron. Mater **2017**, 46, 1339
7. [7] Venkatraman, M.; Neumann, J.P. Bull. Alloy Phase Diagr **1987**, 8, 216
8. [8] He, G.; Zhao, P.; Guo, S.; Chen, Y.; Liu, G. J. Alloys Compd **2013**, 579, 71
9. [9] Hamidi, A.G.; Arabi, H.; Rastegari, S. Int. J. Refract. Met. H **2011**, 29, 538
10. [10] Zhou, K.; Chen, W.G.; Wang, J.J.; Yan, G.J. Int. J. Refract. Met **2019**, H. 82, 91
11. [11] Maiti, K.; Zinzuwadia, M.; Nemade, J. Adv. Mat. Res **2012**, 585, 250
12. [12] Selte, A.; Ozkal, B. Arch. Metall. Mater **2015**, 60 1556
13. [13] Liu, B.; Xie, J.; Qu, X. J. Compos Sci Technol **2008**, 68 1539
14. [13] Hwang, K.S.; Huang, H.S. Mater. Chem. Phys **2001**, 67 92
15. [14] Lahiri, I.; Bhargava, S. Powder Technol **2009** 189, 433
16. [15] Wang, D.; Dong, X.; Zhou, P.; Sun, A. Int. J. Refract. Met H **2016**, 42, 240
17. [16] Wang, D.; Yin, B.; Sun, A.; Li, X.; Qi, C. J. Alloys Compd **2014**, 674, 347
18. [17] Zheng, Z.; Li, X.J.; Gang, T.; Du, C.X. T. Nonferr. Metal. Soc **2009** 19, 626
19. [18] Ibrahim, H.; Aziz, A.; Rahmat, A. Int. J. Refract. Met H **2014** 43, 222
20. [19] Xu, L.; Yan, M.; Xia, Y.; Peng, J.; Li, W.; Zhang, L.; Liu, C. J. Alloys Compd **2014** 592, 202
21. [20] Kim, K.H.; Yoon, W.Y. J. Korean Met. Mater **2016,** 54, 138
22. [21] Ahangarkani, M.; Zangeneh-madar, K. Int. J. Refract. Met H **2018** 75, 1
23. [22] Jiang, K.; Wang, F.; Zhang, J. Rev. Adv. Mater. Sci **2013** 33 322
24. [23] Hakamada, M.; Kuromura, T. J. Mater. Trans **2007** 48, 32
25. [24] Liu, J.; Wang, K. J Mater Sci Technol **2020** 9(2), 2154
26. [25] Hou, C.; Song, X. NPG Asia Mater. **2019** 11, 74